AN INTEGRATED FORWARD-VIEW 2-AXIS MEMS SCANNER FOR COMPACT 3D LIDAR

Dingkang Wang*, Stephan Strassle Rojas, Alexander Shuping, Zaid Tasneem, Sanjeev Koppal, Huikai Xie*
Department of Electrical and Computer Engineering, University of Florida, Gainesville, Florida, USA
*E-mail: noplaxochia@ufl.edu; hkx@ufl.edu

***Abstract*- This paper reports an integrated forward-view 2-axis MEMS scanner that enables ultrasmall 3D LiDAR for applications in micro-air vehicles (MAV). A new design of a pair of vertically-oriented 2-axis scanning MEMS scanner is proposed and fabricated using an innovative fabrication process. Such MEMS scanners are integrated on a silicon optical bench and bent vertically to the substrate, thus forward scan is realized without any beam-folding mirrors. The mirror plate is 0.7 mm × 0.7 mm. The measured optical scan range reaches 17° in both axes at only 4.5 V. The measured resonance frequency of the angular scanning mode is 2.2 kHz. Good optical alignment for LiDAR scanners can be achieved without extra alignment efforts. This MEMS mirror allows a forward-view LiDAR scanner to be monolithically integrated and aligned on a single chip.**

I. INTRODUCTION

In the past two years, LiDAR sensors have drawn great attention in the applications of self-driving vehicles, unmanned air vehicles (UAVs), and ground robotics [1][2][3] for target detection, advanced driver assistance systems (ADAS), and automatic piloted driving. Most of these applications demand low-cost, low-power 3D LiDAR with a small form factor. However, current LiDAR devices are primarily dominated by bulky and relatively slow opto-mechanical scanning-based systems[4]. Thus, reducing the size and weight of optical scanners is crucial. Efforts have been made to miniaturize LiDAR scanners. Particularly, MEMS mirrors have been exploited extensively thanks to their advantages of small size, fast speed and low cost [5][6][7]. For example, Moss *et al.* demonstrated a compact LiDAR system utilizing a MEMS mirror with a 30°×40° field of view (FOV), but this LiDAR still weighed 2.27 kg [8]. Another example is a UVA-borne LiDAR with a MEMS mirror scanner that can fit into a small volume of ~70 mm × 60 mm × 60 mm and weighs ~50 g [1]. But in all those cases, the mirror plates of the MEMS mirrors are parallel to the substrate, so the laser beam must be folded for forward scanning. This requires more components and space as well as extra efforts for precise alignment, making it difficult to further miniaturize LiDAR scanners. It is especially problematic for those insect-sized micro-air vehicles (MAV), such as the RoboBee developed by a research group at Harvard University, which only weighed 80 mg [9][10].

To further reduce the size and weight of forward-view MEMS LiDAR scanners, a highly integrated silicon optical bench (SiOB) with a pair of vertically-oriented micromirrors and a groove for holding a GRIN lens in the aligned position is proposed, designed and fabricated. In the following, the design, fabrication process and device characterization are sequentially described.

II. DEVICE DESIGN

As illustrated in Fig. 1, the proposed LiDAR scanner consists of two vertically-oriented 2-axis micromirrors, an alignment trench, and a GRIN lens, all integrated on a silicon substrate. In contrast, MEMS mirrors for other LiDAR systems typically have their mirror surfaces parallel to the substrate, so multiple assemblies and alignments are required for forward scanning. Thus, the proposed design can greatly simplify the assembly process and drastically reduce the form factor. Either of the 2-axis mirrors can scan in both X and Y directions independently.

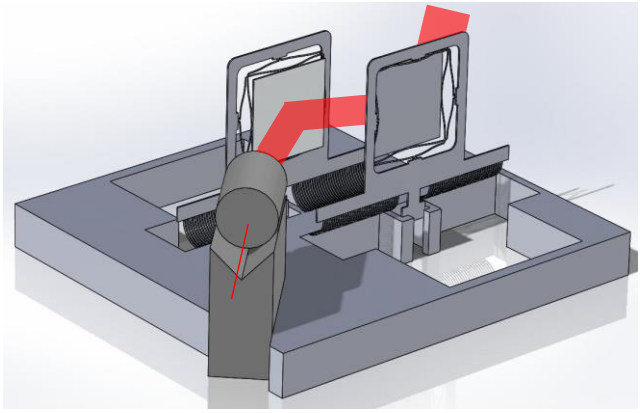

Fig. 1: The proposed optical forward-view scanner integrated on an SiOB.

The 2-axis micromirrors are electrothermally-actuated, based on the inverted-series-connected (ISC) bimorph actuation structure reported in [11]. However, there are two challenges in this design: a) how to ensure the vertical orientation of the micromirrors and b) how to release such complex, out-of-plane microstructures properly. The solution to overcoming the former challenge is discussed in this section and the release process to overcome the latter challenge is presented in Section III.

The optical design of the scanner is shown in Fig. 2. There are two MEMS mirrors in parallel, but the first MEMS mirror is just used as a stationary mirror to fold the laser beam. In order to reduce the form factor, a 0.5 mm-diameter GRIN lens is chosen, which collimates the laser beam to about 0.35 mm in diameter. The laser beam bounces off the first MEMS mirror and is incident on the second MEMS mirror at 45°. The laser spot on

the second MEMS mirror plate is 0.5 mm. When the second MEMS mirror tilts ±5° (or optical angle ±10°), the laser spot on the second mirror plate is increased to 0.54 mm. The mirror plate is designed as 0.7 mm × 0.7 mm so that the entire laser beam is reflected. The distance between the two mirrors is set to 1.3 mm to make sure the laser spot reaches both mirrors without being truncated. If both mirrors actively scan, then the mirror distance and mirror size must be carefully designed to avoid laser beam truncation.

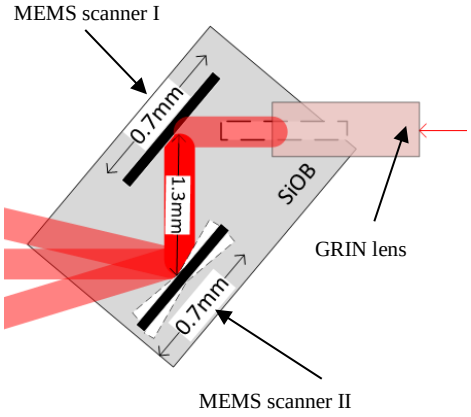

Fig. 2: Optical design of the proposed integrated optical scanner.

A single ISC bimorph actuator design is shown in Fig. 3(a), which consists of three segments: inverted bimorph, overlap, and non-inverted bimorph, leading to zero tangential tip angle θ but with some lateral shift (LS) during actuation. By connecting two ISC actuators in a folded fashion, as shown in Fig. 3(b) and (c), both θ and LS are compensated [11]. In this work, SiO_2 and Al are used as the two bimorph materials while Pt is used as the embedded heater material (not shown).

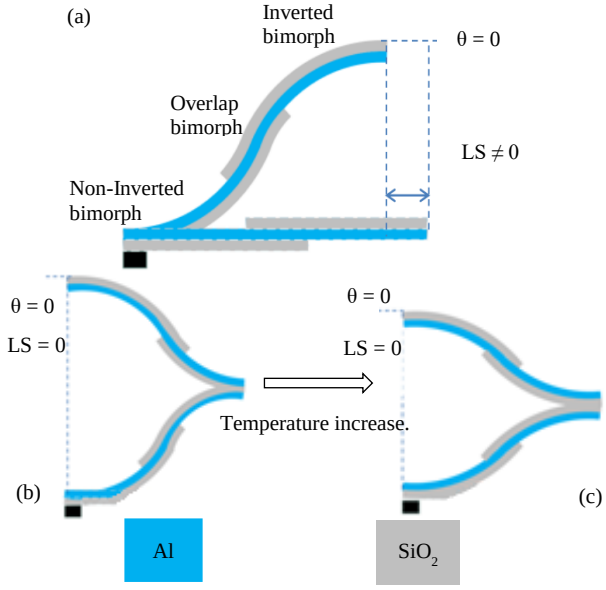

Fig. 3 Principle of the Al/SiO_2 ISC bimorph actuator: (a) One inverse series connected (ISC) bimorph, θ=0, LS≠0. (b) Folded ISC, θ=0, LS=0. (d) Pure vertical displacement with temperature change.

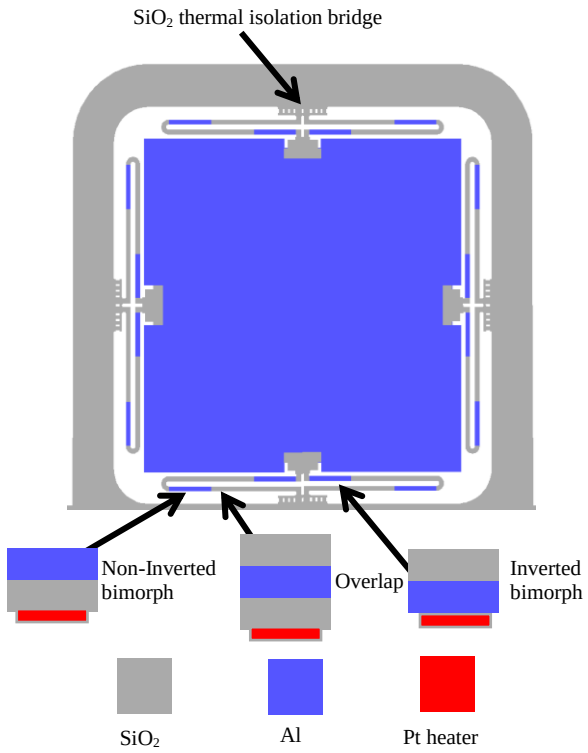

Fig 4. Device topology with the detailed bimorph layer

The topology design of a single MEMS mirror is shown in Fig. 4. COMSOL simulation shows the maximum displacement of the bimorph actuator is expected to be 60 μm at 300°C, which leads to a mechanical tip-tilt angle of 4.5°. Also, according to the simulation, the resonant frequency of the tip-tilt scan mode is 1.5 kHz, assuming a 20 μm thick mirror plate is used.

The mirror frames are pulled up by an array of vertical bending bimorph beams and latched to 90° by a latching mechanism. The design of the latching mechanism is illustrated in Fig. 5, where the tail bar of the mirror frame is stopped by a sidewall of the silicon substrate after the bimorphs are released. The vertical bending bimorph design is shown in Fig. 5, where forty-eight W/SiO_2 bimorphs are used for vertical bending. Each W/SiO_2 bimorph is 21 μm wide and 400 μm long to create over 90° bending angle. The thicknesses of the SiO_2 and W layer are 1 μm and 0.5 μm, respectively, to obtain large bending

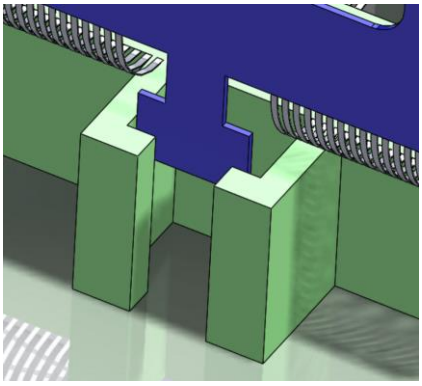

Fig. 5: The stop & latch structure design and W/SiO_2 bending bimorph array.

curvature. The W layer is also used to conduct electrical current to the bimorph actuators of the two MEMS mirrors. The weight of the entire MEMS scanner is 16 mg.

III. Device Fabrication

The fabrication process starts with SOI wafers with a 20 μm-thick device layer, 1 μm-thick buried oxide (BOX) layer and a 500 μm-thick handling layer. First, a 1 μm-thick PECVD SiO_2 layer is deposited and patterned on the front side of the SOI wafer to form the bottom layer for the bimorphs. Then a Cr/Pt/Cr lift-off process is performed to form heaters for the bimorph actuators, followed by sputtering and lift-off a 0.5 μm-thick W layer with high tensile stress for the vertical bending bimorph array. After that, a 0.1 μm PECVD SiO_2 layer is deposited and patterned, and then a 0.9 μm Al layer is sputtered and patterned by a lift-off process to form the other layer of the bimorph actuators. Another 1.2 μm PECVD SiO_2 layer is deposited and patterned by RIE dry etch to form bimorph actuators with SiO_2 as the top layer. The backside Si is DRIE etched with Al_2O_3 as the mask and stops at the BOX layer. Then the BOX layer is removed through RIE.

The release starts with an anisotropic DRIE that etches through the device layer to expose the sidewalls of the silicon underneath the bimorphs, followed by isotropic etching to undercut the silicon blocks to release the bimorphs including both the bimorph actuators and the vertical bending bimorph array. Residual stresses in the thin films of the bimorphs result in initial out-of-plane displacement. The final release step is very challenging. The bimorph actuators must be released before the release of the vertical bending bimorphs. Otherwise, the silicon on the backside of mirror plates and mirror frames will be quickly etched when it is tilted up. The release is achieved by designing the width of the actuator bimorphs smaller than that of the vertical bending bimorphs. Thus, the actuator bimorphs are released before the vertical bending bimorphs start to curl. Continuing the isotropic etching releases the vertical bending beams that bring the two micromirrors to rotate out of the plane. Meanwhile, the latching mechanisms on the frames of the two micromirrors latch the frames at their vertical standing positions.

Fig. 6 shows an SEM of a fabricated device, where the two vertically-oriented micromirrors are each driven by four ISC electrothermal Al/SiO_2 bimorph actuators [11], and the groove for the GRIN lens is 45° to the mirrors. As can be seen from the SEM in Fig. 7(a), the initial elevation of the mirror plate is about 155 μm and the mirror plate is parallel to the mirror frame. The actuators form dual-S-shaped structures because of the residual stress. Details of the bent W/SiO_2 bimorph array and the stopper and latch structure are shown in the SEMs in Figs. 7(b).

IV. Device Characterization

The measured static scan response and frequency response are plotted in Figs. 8(a) and (b), where an optical scan range of ±8.5° is obtained at 4.5 Vdc for both axes. The linear scan range is from 1° to 8.5°. The first resonant mode occurs at 1.03 kHz,

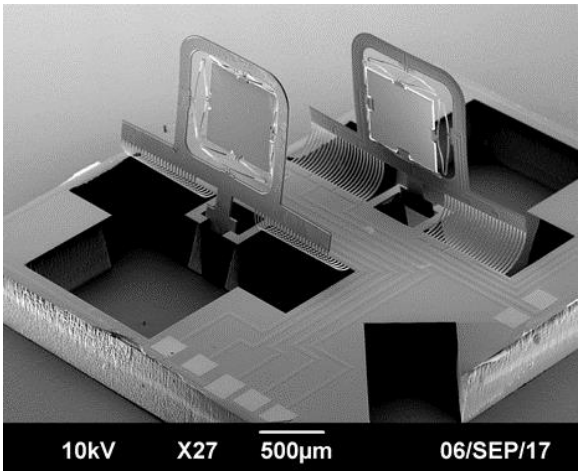

Fig. 6: SEM of the fabricated MEMS scanner.

which is identified as the frame rotation mode. The stiffness of the bimorph array is more than 20× greater than that of the Al/SiO_2 bending bimorph array reported in a previous work [12] because of Young's modulus of W is much higher than that of Al. The tip-tilt angular scan mode is at 2.2 kHz, which is greater than the designed 1.5 kHz. This increased resonance frequency is attributed to the mirror plate thinned down by the last DRIE release step. A step response measurement shows that the measured rise time is 2.4 ms.

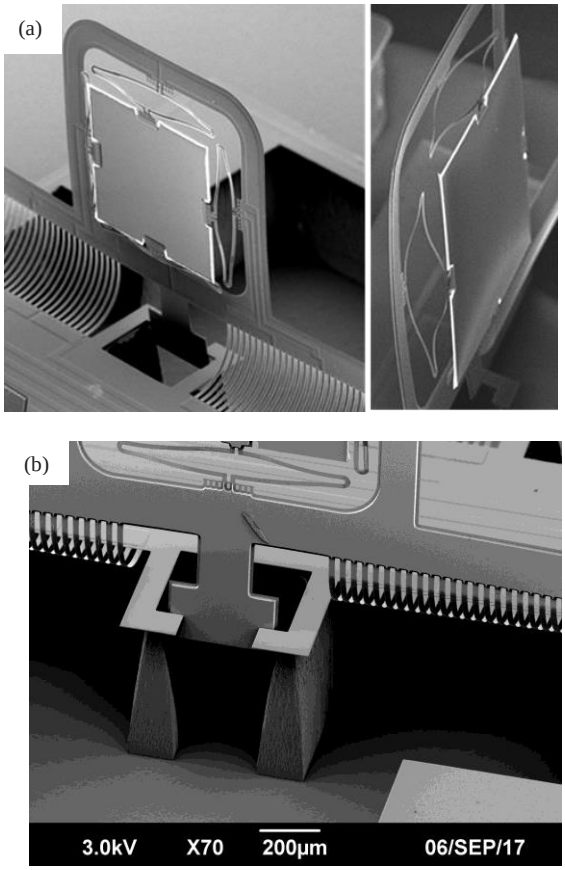

Fig. 7: (a) An SEM of one MEMS mirror with Al/SiO_2 bimorph actuators. (b) An SEM of the bent W/SiO_2 bimorph array and stop & latch structure.

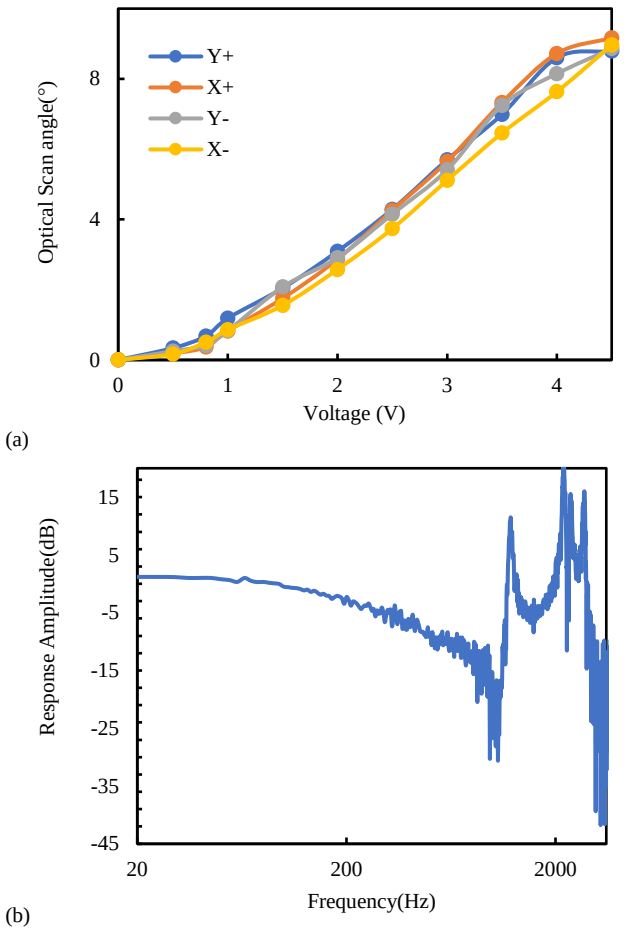

Fig. 8: Static response (a) and frequency response (b) of the MEMS scanner.

LiDAR ranging measurement was also conducted with a Lightware OSLRF-01 LiDAR module. The MEMS mirror was driven with a 0.2 Hz 2 V triangle wave. The MEMS based module was used to scan a step of 7.5 cm. The peak power of the laser pulse (905 nm) was 14 W with a pulse width of 30 ns. The result is shown in Fig. 9, where the step is clearly delineated. The resolution is about 3.6 cm. Also note that the OSLRF-01 uses a technique called sequential-equivalent-time-sampling (SETS), with which ADCs at a sampling rate of 16 kHz is adequate to acquire the ZERO and RETURN pulse signals.

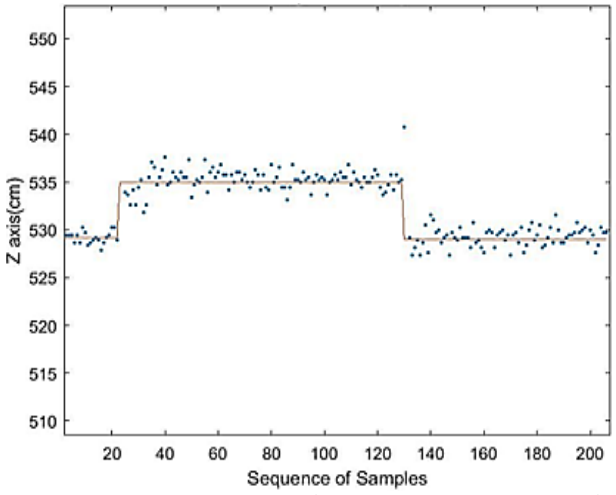

Fig 9: LiDAR measurement data of MEMS mirror scanning a step of 7.5 cm.

V. Conclusion

An integrated forward-view 2-axis MEMS scanner with a large FOV of 17° has been successfully demonstrated. Two vertically-oriented MEMS mirrors are integrated on an SiOB, forming an ultra-compact forward-view optical scanner. The vertical standing is warranted by W/SiO_2 bimorphs and a special latching mechanism. The forward-view scanner (with a GRIN lens included) has a form factor of only 4 mm × 4.5 mm × 1.6 mm and weighs just 16 mg. This novel, compact forward-view scanner is ideal for MAVs and has a great potential for applications in insect-sized MAVs.

Acknowledgment

This work is supported by the National Science Foundation under the award#1514154 and by the National Natural Science Foundation of China (No. 61528401).

References

[1] Kasturi, Abhishek, Veljko Milanovic, Bryan H. Atwood, and James Yang. "UAV-borne lidar with MEMS mirror-based scanning capability." In Proc. SPIE, vol. 9832, p. 98320M. 2016.

[2] Niclass, Cristiano, Kota Ito, Mineki Soga, Hiroyuki Matsubara, Isao Aoyagi, Satoru Kato, and Manabu Kagami. "Design and characterization of a 256x64-pixel single-photon imager in CMOS for a MEMS-based laser scanning time-of-flight sensor." Optics Express 20, no. 11 (2012): 11863-11881.

[3] Stann, Barry L., John F. Dammann, and Mark M. Giza. "Progress on MEMS–scanned Ladar." In Proc. SPIE, vol. 9832, p. 98320L. 2016.

[4] http://www.renishaw.com/en/optical-encoders-and-lidar-scanning--39244

[5] Holmstrom, Sven TS, Utku Baran, and Hakan Urey. "MEMS laser scanners: a review." *Journal of Microelectromechanical Systems* 23, no. 2 (2014): 259-275.

[6] Hofmann, Ulrich, and Joachim Janes. "MEMS mirror for low cost laser scanners." *Advanced Microsystems for Automotive Applications 2011* (2011): 159-165.

[7] Wang, Dingkang, Xiaoyang Zhang, Liang Zhou, Mengyue Liang, Daihua Zhang, and Huikai Xie. "An ultra-fast electrothermal micromirror with bimorph actuators made of copper/tungsten." In *Optical MEMS and Nanophotonics (OMN), 2017 International Conference on*, pp. 1-2. IEEE, 2017.

[8] Moss, Robert, Ping Yuan, Xiaogang Bai, Emilio Quesada, Rengarajan Sudharsanan, Barry L. Stann, John F. Dammann, Mark M. Giza, and William B. Lawler. "Low-cost compact MEMS scanning ladar system for robotic applications." In *Proc. SPIE*, vol. 8379, p. 837903. 2012.

[9] Floreano, Dario, and Robert J. Wood. "Science, technology and the future of small autonomous drones." *Nature* 521, no. 7553 (2015): 460-466.

[10] Ma, Kevin Y., Pakpong Chirarattananon, Sawyer B. Fuller, and Robert J. Wood. "Controlled flight of a biologically inspired, insect-scale robot." *Science* 340, no. 6132 (2013): 603-607.

[11] Jia, Kemiao, Sagnik Pal, and Huikai Xie. "An electrothermal tip–tilt–piston micromirror based on folded dual S-shaped bimorphs." *Journal of Microelectromechanical systems* 18, no. 5 (2009): 1004-1015.

[12] Duan, Can, Wei Wang, Xiaoyang Zhang, Liang Zhou, Antonio Pozzi, and Huikai Xie. "A Self-Aligned 45°-Tilted Two-Axis Scanning Micromirror for Side-View Imaging." *Journal of Microelectromechanical Systems* 25, no. 4 (2016): 799-811.